The Canadian Mineralogist
Vol. 33, pp. 1131-1151 (1995)

BORATE MINERALS. I. POLYHEDRAL CLUSTERS AND FUNDAMENTAL BUILDING BLOCKS

PETER C. BURNS*

Department of Earth Sciences, University of Cambridge, Downing Street, Cambridge CB2 3EQ, U.K.

JOEL D. GRICE

Research Division, Canadian Museum of Nature, P.O. Box 3443, Station D, Ottawa, Ontario K1P 6P4

FRANK C. HAWTHORNE

Department of Geological Sciences, University of Manitoba, Winnipeg, Manitoba R3T 2N2

Abstract

In general, the structures of the borate minerals are based on $B\phi_3$ and $B\phi_4$ polyhedra, which occur as discrete oxyanions or polymerize to form finite clusters, chains, sheets and frameworks. The B-ϕ bonds (ϕ: unspecified anion) are of much higher bond-valence than the interstitial bonds, and thus borate minerals readily lend themselves to hierarchical classification based on the topological character of the FBB (fundamental building block) and the structural unit. Here, we derive topologically and metrically possible finite clusters of the form $[B_n\phi_m]$, where $3 \le n \le 6$, and identify those clusters that occur as FBBs of the structures of borate minerals. In addition, we have developed graphical and algebraic descriptors of the topological and chemical aspects of the clusters and their mode of polymerization. In the structures of the borate minerals based on FBBs with $3 \le n \le 6$, all FBBs are polyhedral rings or decorated polyhedral rings. Moreover, three-membered polyhedral rings are almost completely dominant; the only exception is the four-membered polyhedral ring in borcarite. Three-membered polyhedral rings occur in the following order of preference: <Δ2□> >> <2Δ□> > <3□> > <3Δ>. Only a small number of the topologically and metrically possible clusters occur as FBBs in borate minerals; Nature seems to produce structural diversity by using only a small number of FBBs and then polymerizing them in many different ways.

Keywords: borate minerals, hierarchy of structures, fundamental building block, crystal structure, boron, structure classification.

Sommaire

En général, les structures des minéraux boratés ont comme unités de base des polyèdres $B\phi_3$ et $B\phi_4$, présents sous forme d'anions distincts ou en agencements polymérisés, qui sont soit des regroupements limités de polyèdres, des chaînes, des feuillets ou des trames. Les liaisons B–ϕ (ϕ: anion non spécifié) possèdent une valence de liaison beaucoup plus élevée que les liaisons interstitielles, de telle sorte que les minéraux boratés se prêtent tout naturellement à un schéma de classification hiérarchique fondé sur le caractère topologique du bloc structural fondamental et de l'unité structurale de base. Nous dérivons ici tous les agencements finis possibles selon les critères topologiques et métriques appropriés pour les agencements de type $[B_n\phi_m]$, dans lesquels $3 \le n \le 6$, et nous identifions les agencements qui servent de bloc structural fondamental dans les structures de minéraux boratés. En plus, nous développons les attributs graphiques et algébriques requis pour décrire les aspects topologiques et chimiques des agencements et leur mode de polymérisation. Dans toute structure d'un minéral boraté impliquant un bloc structural fondamental avec $3 \le n \le 6$, ce bloc constitue un anneau de polyèdres, décoré ou non. De plus, les anneaux à trois membres sont fortement prédominants. La seule exception, en fait, est la borcarite, qui contient un anneau à quatre polyèdres. Les anneaux à trois polyèdres se rencontrent avec une fréquence dans l'ordre <Δ2□> >> <2Δ□> > <3□> > <3Δ>. Les minéraux boratés ne contiennent qu'un nombre restreint des agencements topologiquement et métriquement possibles. La diversité structurale s'explique donc par un petit nombre de blocs structuraux fondamentaux, qui sont polymérisés de plusieurs façons dans les structures.

(Traduit par la Rédaction)

Mots-clés: minéraux boratés, hiérarchie des structures, bloc structural fondamental, structure cristalline, bore, classification structurale.

---

* Present address: Department of Earth and Planetary Sciences, University of New Mexico, Albuquerque, New Mexico 87131-1116, U.S.A.

INTRODUCTION

Boron has an ionic radius of 0.11 Å (Shannon 1976), and hence can occur in both triangular and tetrahedral coordination where bonded to oxygen. $B\phi_3$ (ϕ: O^{2-}, OH^-) groups have an average B–ϕ bond-valence approximately equal to 1 valence unit (v.u.), and $B\phi_4$ groups have an average B–ϕ bond-valence approximately equal to ¾ v.u. Hence, both $B\phi_3$ and $B\phi_4$ groups can polymerize by sharing corners without violating the valence-sum rule (Brown 1981). Such polymerization is very common in both minerals and synthetic inorganic compounds, and gives rise to great structural diversity. In general, a borate structure contains clusters of corner-sharing $B\phi_3$ and $B\phi_4$ polyhedra, which occur as discrete polyanions or polymerize to form larger clusters, chains, sheets or frameworks. The excess charge of the array of borate polyhedra is balanced by the presence of low-valence interstitial cations. In the structures of most borate minerals, the B–ϕ bonds are of much higher bond-valence ($\geq$ 0.7 v.u.) than the remaining cation–ϕ bonds ($\leq$ 0.3 v.u.). Thus, the borate structures readily lend themselves to classification on the basis of the geometry of the clusters of borate polyhedra.

The utility of organizing crystal structures into hierarchical sequences has long been recognized. Bragg (1930) first classified the silicate structures according to the geometry of the polymerization of the $(Si,Al)O_4$ tetrahedra, and this scheme was generalized to include structures based on polymerized tetrahedra by Zoltai (1960) and Liebau (1985). Such hierarchical classifications serve to order our knowledge and to facilitate comparison of crystal structures, which is intrinsically quite difficult. However, much additional insight can be derived from such structural schemes, particularly regarding the underlying controls on bond topology (Hawthorne 1983, 1994) and mineral paragenesis (Moore 1965, 1973, Hawthorne 1984). There have been several classifications proposed specifically for borate structures (Edwards & Ross 1960, Christ 1960, Tennyson 1963, Ross & Edwards 1967, Heller 1970, Christ & Clark 1977). Previous classifications were reviewed by Christ & Clark (1977). Their classification has proven very useful over the past fifteen years, and has been widely used. The basis of the Christ & Clark (1977) scheme is the degree of polymerization within the simplest structural unit. They portrayed this with the descriptor $n{:}i\Delta + jT$, where n is the total number of boron atoms within this unit, which contains i $B\phi_3$ and j $B\phi_4$ polyhedra. Although this is useful information, it does not give any indication about the topology of the cluster of polyhedra nor about the degree to which the cluster is translated throughout the crystal structure. These two structural features are the ones we incorporate in the present scheme of classification, as they are essential to the understanding of the hierarchy of the borate structures and, ultimately, the paragenesis of borate minerals.

The scheme of Christ & Clark (1977)

In their crystal-chemical classification of borate structures, Christ & Clark (1977) emphasized the importance of polymerization of $B\phi_3$ triangles and $B\phi_4$ tetrahedra to form clusters that are compact, insular groups, referred to as *fundamental building blocks* (FBB). The FBBs form the basis of the classification scheme of Christ & Clark (1977). Their structural classification is based on three principal criteria: (1) the number of boron atoms in the FBB, (2) the number of $B\phi_3$ triangles and $B\phi_4$ tetrahedra in the FBB, and (3) the mode of polymerization between the FBBs, giving isolated, modified isolated, chains, modified chains, sheets and modified sheets. Christ & Clark (1977) proposed a notation ($n{:}i\Delta + jT$) for each FBB, which gives the total number of boron atoms in the FBB, as well as the number of $B\phi_3$ triangles (Δ) and $B\phi_4$ tetrahedra (T). For example, the FBB $5{:}2\Delta{+}3T$ has five boron atoms in the FBB, of which two occur as $B\phi_3$ triangles, and three as $B\phi_4$ tetrahedra.

The occurrence of large FBBs

In developing their classification, Christ & Clark (1977) considered the structures of the hydrous borate minerals available at that time, as well as the structures of some anhydrous minerals and hydrous and anhydrous synthetic inorganic compounds. They noted that the FBBs of borate structures are generally small, as nearly all structures known at that time were based upon FBBs with six or less boron atoms. The one exception was preobrazhenskite, the structure of which is based on FBBs containing nine boron atoms. Since the work of Christ & Clark (1977), however, several borate structures that contain even larger FBBs have been reported. Grice *et al.* (1994) solved the structures of pringleite $\{Ca_9[B_{20}O_{28}(OH)_{18}][B_6O_6(OH)_6]\cdot 13H_2O\}$ and ruitenbergite $\{Ca_9[B_{20}O_{28}(OH)_{18}][B_6O_6(OH)_6]\cdot 13H_2O\}$, both of which contain FBBs with 12 boron atoms. Several synthetic compounds have 12 or more boron atoms in the FBB [*i.e.*, $Ag_6[B_{12}O_{18}(OH)_6]\cdot 3H_2O$ (Skakibaie-Moghadam *et al.* 1990), $Na_8[B_{12}O_{20}(OH)_4]$ (Menchetti & Sabelli 1979), $Na_6[Cu_2\{B_{16}O_{24}(OH)_{10}\}]\cdot 12H_2O$ (Behm 1983), $K_6[UO_2\{B_{16}O_{24}(OH)_8\}]\cdot 12H_2O$ (Behm 1985), and $K_5H\{Cu_4O[B_{20}O_{32}(OH)_8]\}\cdot 33H_2O$ (Heller & Pickardt 1985)]. These more complex structures present a problem for the Christ & Clark (1977) scheme of classification, which cannot uniquely distinguish FBBs with its nomenclature. For example, the FBBs with twelve boron atoms in pringleite, ruitenbergite, $Na_8[B_{12}O_{20}(OH)_4]$ and $Ag_6[B_{12}O_{18}(OH)_6]\cdot 3H_2O$ all contain six $B\phi_3$ triangles and six $B\phi_4$ tetrahedra, and the notation for these FBBs is thus $12{:}6\Delta{+}6T$. However, examination of the FBBs of these

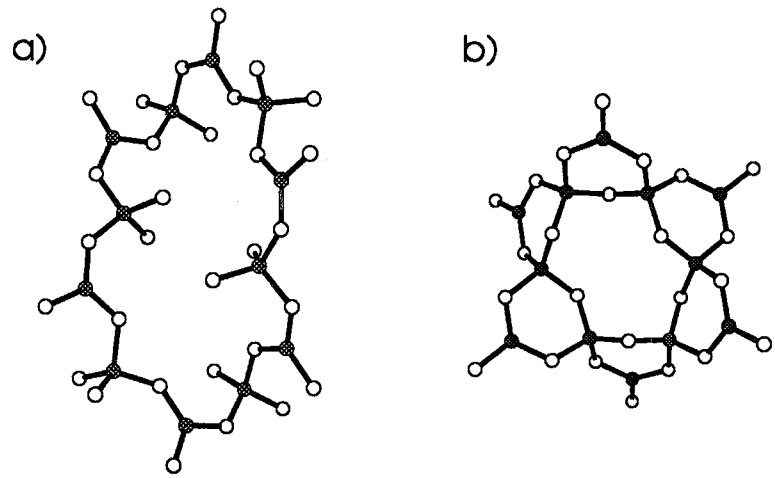

FIG. 1. Examples of the FBB 12:6Δ+6T; a) pringleite, b) $Na_8[B_{12}O_{20}(OH)_4]$.

structures (Fig. 1) shows that the FBBs in pringleite and ruitenbergite are twelve-membered rings of polyhedra with alternating $B\phi_3$ triangles and $B\phi_4$ tetrahedra, whereas the FBBs in $Na_8[B_{12}O_{20}(OH)_4]$ and $Ag_6[B_{12}O_{18}(OH)_6]\cdot 3H_2O$ each contain six three-membered rings of polyhedra containing $B\phi_4$ tetrahedra and one $B\phi_3$ triangle, and these rings form a larger ring by sharing $B\phi_4$ tetrahedra (Fig. 1). In the classification of Christ & Clark (1977), structures based on FBBs with identical numbers of $B\phi_3$ triangles and $B\phi_4$ tetrahedra always have identical descriptors, even where the structural arrangements are very different; their notation does not indicate the topological characteristics of their linkage. This is of general significance; Burdett (1986) has shown that the energy difference between two structures can be expressed in terms of the first few disparate moments of the electronic energy density-of-states of the two structures. In structural terms (Hawthorne 1994), the important terms in the formulation of energy involve differences in coordination number [which are described in the notation scheme of Christ & Clark (1977)] and differences in local linkage of the polyhedra [which are *not*]. Thus it is desirable to incorporate information on local linkage of polyhedra into a description of FBBs.

A PROPOSED DESCRIPTOR FOR FUNDAMENTAL BUILDING BLOCKS IN BORATES

In this series of papers, we intend to develop a hierarchy of borate structures based on a FBB that we define as a strongly bonded cluster of borate polyhedra that is repeated by the translational symmetry operators to give the structural unit (Hawthorne 1983, 1985). As a part of the development of the hierarchy of borate structures, a descriptor for borate FBBs that includes information on connectivity of the polyhedra is required. In developing such a descriptor, it is necessary to strike a balance between the amount of information conveyed and the complexity of the descriptor. Although our method does not always result in a unique descriptor for the FBB, considerably more information is included than in previous schemes.

B–B graphs

The representation of large polyhedral clusters is considerably simplified by omitting the anions, as is common in topological considerations of crystal structures (Smith 1977, 1988, Hawthorne 1983, 1990). Such graphs are used to show B–B connectivity relationships; B–ϕ–B bonds are shown as a single line connecting the boron atoms, and nonbridging anions are omitted completely. Information on the coordination number of the boron atoms is retained by using different symbols (Δ and □) for the nodes of the graph. B–B graphs are used extensively in this paper; examples are shown in Figure 2, where they may be compared with the conventional representations involving all the atoms of the cluster.

FBB descriptor

Borate FBBs must contain either $B\phi_3$ triangles or $B\phi_4$ tetrahedra, or both. Examination of borate structures shows that many FBBs also contain *rings* of $B\phi_n$ polyhedra. The importance of three-membered rings is striking; almost all large FBBs contain these rings. Thus, it is necessary that the descriptor also denotes the occurrence of rings in the FBBs.

The FBB descriptor proposed here is based on: (1)

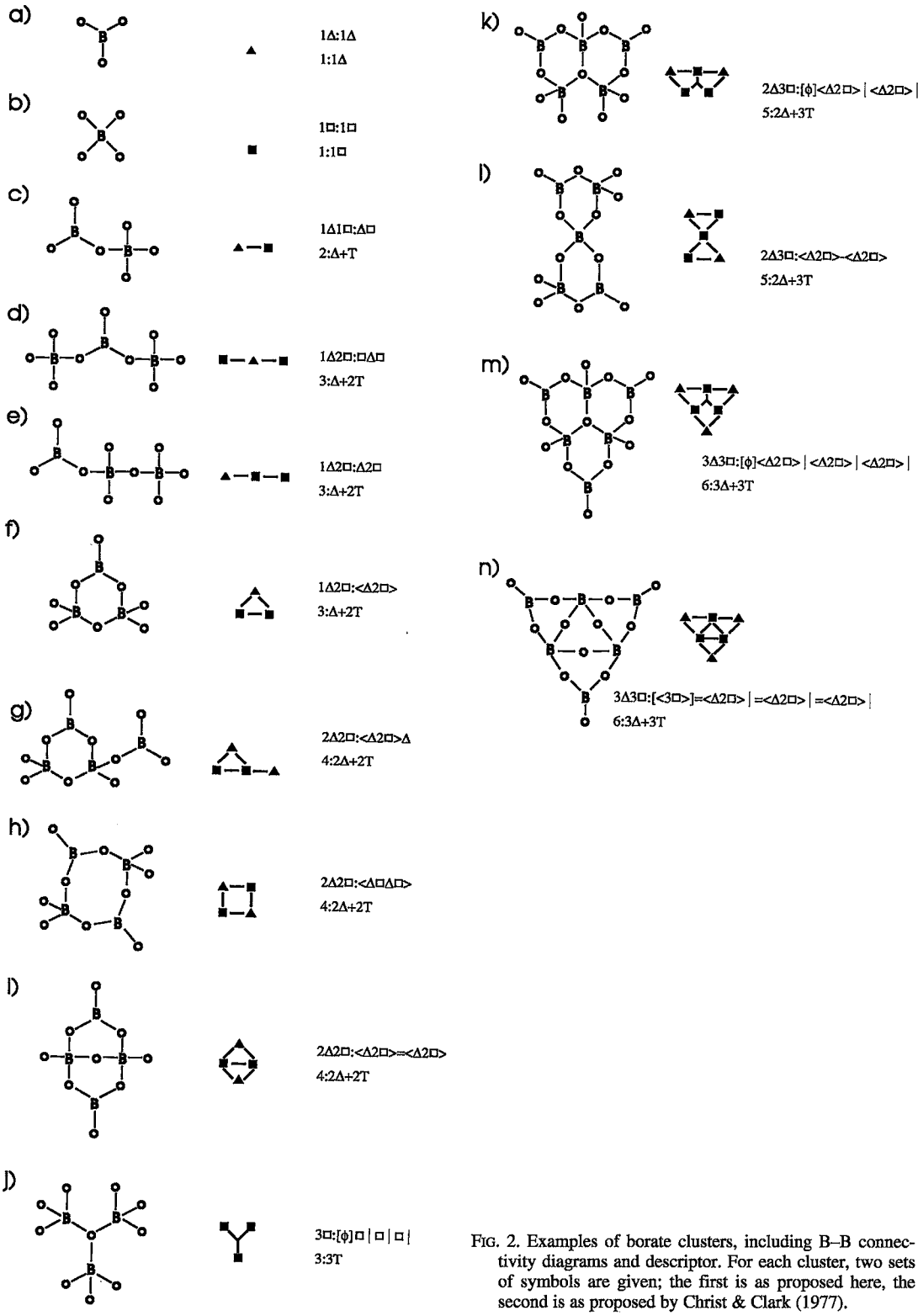

FIG. 2. Examples of borate clusters, including B–B connectivity diagrams and descriptor. For each cluster, two sets of symbols are given; the first is as proposed here, the second is as proposed by Christ & Clark (1977).

the number of borate polyhedra in the FBB, (2) the number of $B\phi_3$ triangles and $B\phi_4$ tetrahedra in the FBB, (3) the connectivity of the polyhedral groups in the FBB, (4) the presence of rings in the FBB, and (5) the connectivity of the rings within the FBB. The descriptor has the general form *A:B*, where *A* is the number of $B\phi_3$ triangles and $B\phi_4$ tetrahedra in the FBB, and *B* is a character string that contains the information for points (3) to (5) above.

Numbers of borate polyhedra in the FBB

In many cases, the numbers of $B\phi_3$ triangles and $B\phi_4$ tetrahedra in the FBB are uniquely defined by the character string *B*. However, for some of the larger FBBs, the character string only uniquely defines the total number of borate polyhedra in the FBB and not the numbers of $B\phi_3$ triangles and $B\phi_4$ tetrahedra. Symbol *A* of the descriptor gives the numbers of $B\phi_3$ triangles (Δ) and $B\phi_4$ tetrahedra (□) in the form $i\Delta j\square$, where *i* and *j* are integers representing the number of $B\phi_3$ triangles and $B\phi_4$ tetrahedra, respectively.

Linkage between borate polyhedra in the FBB

Simple linkage: The simplest FBBs contain only one $B\phi_3$ triangle or $B\phi_4$ tetrahedron, and *A:B* is written as 1Δ:Δ or 1□:□ (Figs. 2a,b). Many FBBs contain more than one borate polyhedron, and polymerization of adjacent polyhedra involves corner-sharing only. Borate polyhedra (symbolized by Δ and □) that share corners within the FBB occur adjacent to each other in the FBB descriptor. Thus, a FBB written as 1Δ1□:Δ□ contains one $B\phi_3$ triangle and one $B\phi_4$ tetrahedron that share one anion (Fig. 2c). Where more than two polyhedra occur in the FBB, the order in which the symbols are written should be consistent with the linkage in the FBB. Compare 1Δ2□:□Δ□ and 1Δ2□:Δ□□ (Figs. 2d,e); in the first case, the central $B\phi_3$ triangle shares an anion with each of two $B\phi_4$ tetrahedra; in the second case, the central $B\phi_4$ tetrahedron shares a ligand with a $B\phi_3$ triangle on one side, and a $B\phi_4$ tetrahedron on the other. The new descriptor distinguishes between these two cases (Figs. 2d,e).

Rings of polyhedra: Rings of either or both □ and Δ occur in most FBBs that contain three or more borate polyhedra. Where the polyhedra share vertices to form a ring, the ring is enclosed in the delimiters < >. For example, the FBB 1Δ2□:<Δ2□> contains one $B\phi_3$ triangle and two $B\phi_4$ tetrahedra that share anions to form a three-membered ring (Fig. 2f). Some clusters contain a number of polyhedral rings of various sizes, which generates some ambiguity in developing the descriptor of the cluster. Such clusters will be described using the smallest possible rings that permit a full description of the cluster; in most cases, these will contain only three or four polyhedra. Such rings as <Δ2□> commonly link to one or more Δ or □ or to other rings. The FBB 2Δ2□:<Δ2□>Δ has such a linkage (Fig. 2g). Compare the FBB 2Δ2□:<Δ□Δ□>, a four-membered ring of alternating Δ and □ (Fig. 2h); the proposed descriptor distinguishes these clusters.

Linkage of rings of polyhedra: Where two rings are linked together, the number of borate polyhedra that the two rings have in common is indicated by –, =, ≡, *etc.* for one, two, three or more polyhedra, respectively. The FBB 2Δ2□:<Δ2□>=<Δ2□> contains two <Δ2□> rings, and the rings have two borate polyhedra in common (Fig. 2i). This particular linkage shows why the *A* part of the descriptor is required. It can be shown (Appendix A1) that there are nine possible arrangements of four borate polyhedra that consist of two three-membered rings with two polyhedra in common, as illustrated in Figure 3. Clusters 3a and 3i are obviously distinct in all aspects of their topology and descriptor. Clusters 3d, 3e and 3f have the same *A* symbol (2Δ2□) and hence the same stoichiometry, yet they have a different topology. Cluster 3d consists of two <2Δ□> rings that have two $B\phi_3$ triangles in common, cluster 3e consists of two <Δ2□> rings that have two $B\phi_4$ tetrahedra in common, and cluster 3f has both a <2Δ□> and a <Δ2□> ring, which have a $B\phi_3$ triangle and $B\phi_4$ tetrahedron in common; the *B* symbol distinguishes clusters 3d, 3e and 3f. Clusters 3b and 3d have the same *B* symbol but have different stoichiometry and topology; cluster 3b consists of two <2Δ□> rings with a $B\phi_3$ triangle and a $B\phi_4$ tetrahedron in common, whereas cluster 3d consists of two <2Δ□> rings with two $B\phi_3$ triangles in common. The *A* symbol distinguishes clusters 3b and 3d. Only a *combination* of the *A* and *B* symbols can distinguish all possible topological linkages involving four polyhedra with two three-membered rings and two shared polyhedra.

[n]-connected anions, polyhedra and rings: In borate structures, most oxygen atoms are not bonded to more than two boron atoms. However, in some cases, an oxygen atom is bonded to three boron atoms (*e.g.*, tunellite: Burns & Hawthorne 1994a) or four boron atoms (*e.g.*, the high-temperature form of boracite, Sueno *et al.* 1973). Also, borate polyhedra may be connected to more than two other polyhedra, and rings of polyhedra may be connected to many other polyhedra or rings of polyhedra. The descriptor developed above does not permit the descriptions of these possibilities, as any one symbol in the linear character string (*B*) cannot be more than [2]-connected. It is necessary to introduce further descriptors for such clusters.

Any anion (ϕ), polyhedron, or ring of polyhedra that is more than [2]-connected in the character string *B* may be enclosed in the delimiters [ ]. For example, an anion connected to three borate polyhedra is [ϕ], whereas a ring of three corner-sharing $B\phi_4$ tetrahedra

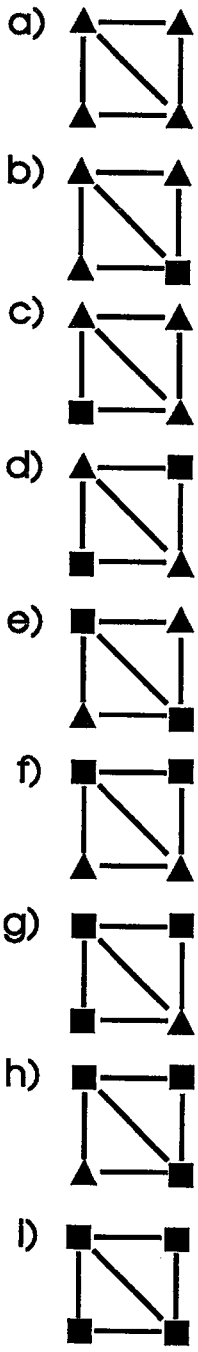

FIG. 3. Possible clusters of four borate polyhedra that contain two three-membered rings with two polyhedra in common.

that is [3]-connected is [<3□>]. A list of the polyhedra or clusters that are connected to the central unit follows the [ ] delimiters; each cluster that is separately connected to the central unit is terminated by the symbol |; note that the order of the listing of these clusters is not important.

Consider an oxygen atom that is shared among three $B\phi_4$ tetrahedra (Fig. 2j). The descriptor for this cluster is 3□:[ϕ]□ | □|□|, indicating that it contains three $B\phi_4$ tetrahedra, each of which is connected to a central anion. The cluster given in Figure 2k also contains an oxygen atom that is shared among three $B\phi_4$ tetrahedra. In this case, the cluster also contains two <Δ2□> rings that have one $B\phi_4$ tetrahedron in common. The descriptor is 2Δ3□:[ϕ]<Δ2□>|<Δ2□>|; note that the sharing of one $B\phi_4$ tetrahedron between the <Δ2□> rings is not explicitly indicated in the descriptor, but as the cluster only contains three $B\phi_4$ tetrahedra, the rings must share one $B\phi_4$ tetrahedron. For the cluster given in Figure 2l, the descriptor is 2Δ3□:<Δ2□>–<Δ2□>, and there are two rings of polyhedra that have one $B\phi_4$ tetrahedron in common, but with no [ϕ] anion present.

Two clusters that contain six borate polyhedra are shown in Figures 2m and 2n, but the connectivity of these clusters is quite different. In Figure 2m, the cluster contains three <Δ2□> rings, of which each is connected to a central oxygen atom. The descriptor is 3Δ3□:[ϕ]<Δ2□>|<Δ2□>|<Δ2□>|, which indicates that three <Δ2□> rings share a central anion; as the cluster contains 3Δ3□, each ring must have two $B\phi_4$ tetrahedra in common with other rings. The cluster in Figure 2n also contains 3Δ3□, but in this case there are four three-membered rings of polyhedra, one <3□> and three <Δ2□>. The central <3□> ring connects to the three <Δ2□> rings by sharing two borate polyhedra, and thus the descriptor is 3Δ3□:[<3□>]=<Δ2□>|=<Δ2□>|=<Δ2□>|.

Large FBBs

The new descriptor effectively distinguishes between the larger FBBs in phases such as pringleite, ruitenbergite, $Na_8[B_{12}O_{20}(OH)_4]$ and $Ag_6[B_{12}O_{18}(OH)_6]\cdot 3H_2O$ (Fig. 1). The FBBs in pringleite and ruitenbergite are 6Δ6□:<□Δ□Δ□Δ□Δ□Δ□Δ>, indicating that they are twelve-membered rings of polyhedra made of an alternation of $B\phi_4$ tetrahedra and $B\phi_3$ triangles. The FBBs in $Na_8[B_{12}O_{20}(OH)_4]$ and $Ag_6[B_{12}O_{18}(OH)_6]\cdot 3H_2O$ are 6Δ6□: <<Δ2□>–<Δ2□>–<Δ2□>–<Δ2□>–<Δ2□>–<Δ2□>–>, indicating that the FBB contains six three-membered rings of polyhedra, each of which contain one $B\phi_3$ triangle and two $B\phi_4$ tetrahedra; these six rings link to form a larger ring of <Δ2□> units (Fig. 1). The *B* strings are rather cumbersome in this form; they may be condensed in a very simple fashion by noting that the symbol has translational symmetry. It is common in

mathematics to represent a repeating string of figures by the symbol • (*e.g.*, ⅓ = 0.333•). We can use a similar symbolism here. The unique sequence is written, followed by the symbol • to show that it repeats to the length of the *B* string as indicated by the *A* term. Thus 6Δ6□:<□Δ□Δ□Δ□Δ□Δ□Δ> becomes 6Δ6□:<□Δ•>, and 6Δ6□:<<Δ2□>–<Δ2□>–<Δ2□>–<Δ2□>–<Δ2□>–<Δ2□>–> becomes 6Δ6□:<<Δ2□>–•>.

Hydrogen Bonding

The majority of borate minerals are hydrous, and hydrogen bonding is ubiquitous in these structures (*e.g.*, Burns & Hawthorne 1993a, b, 1994a, b, c, d, 1995). In some cases (*e.g.*, Grice *et al.* 1994), it is desirable to include information on the identities of the anions in the FBB. In general, borate triangles and tetrahedra are $BO_{3-n}(OH)_n$ and $BO_{4-n}(OH)_n$, respectively, and the symbols for borate triangles and tetrahedra in the descriptor may be modified by adding *n* as a superscript, giving the symbols Δ^n and $\square^n$.

Tabulation of Polyhedral Clusters to $n = 6$

Most FBBs contain six or less borate polyhedra, although there are exceptions. Upon examination of possible clusters of polyhedra, it is apparent that there are many topologically possible clusters of six or less borate polyhedra that have not yet been observed as FBBs in a mineral or an inorganic compound. This may be due to the relatively small size of the sample (the structures of 102 minerals are known); for example, the 4□:<4□> FBB has only been identified in borcarite (Burns & Hawthorne 1995). In other cases, the postulated arrangement of borate polyhedra may be energetically unfavorable. One of the goals of this work is to identify all topologically possible clusters (within certain imposed boundary-constraints) without specific emphasis placed upon those clusters (*i.e.*, FBBs) that have already been observed in minerals.

Enumeration of possible clusters

In deriving possible borate clusters, we consider only $B\phi_3$ and $B\phi_4$ polyhedra. As edge- or face-sharing borate polyhedra have not been observed, we consider only corner-sharing between borate polyhedra. We omit clusters with any [1]-connected polyhedra; thus chains (there are seventy-one chains for $3 \le n \le 6$) and *decorated* clusters are not included. Here, we limit tabulation to clusters in which all borate polyhedra are at least [2]-connected. Thus we include the clusters 3□:<3□> and 1Δ2□:<Δ2□>, but exclude 4□:<3□>□ and 1Δ3□:<Δ2□>□, considering the [1]-connected polyhedra as decorations on the cluster to which they link.

Initially, all geometrically possible clusters (with the exceptions listed above) were derived as shown in Appendix A2, with the (temporary) restriction that these clusters contain only □; the complete set of clusters can then be derived by permuting □ and Δ. These thirty-nine clusters are given in Figures 4 and 5, along with the corresponding B–B graphs and their descriptors.

Some of the clusters permit considerable flexibility in selecting a suitable descriptor. In these cases, the symbols of the descriptor are organized so as to emphasize the presence of the smallest rings within the larger cluster, while still giving a complete description of the cluster. We recommend that the form of the descriptor in Figures 4 and 5 be adopted in general,

Fig. 4a

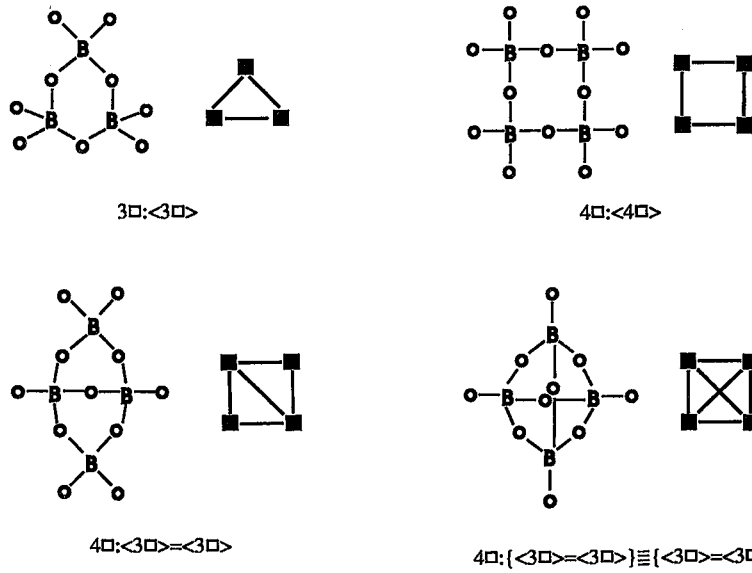

Fig. 4b

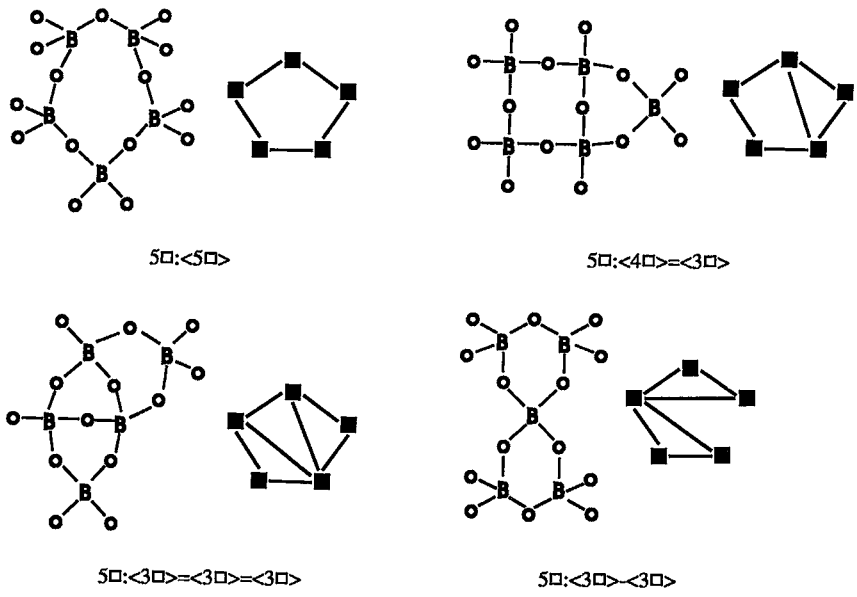

Fig. 4c

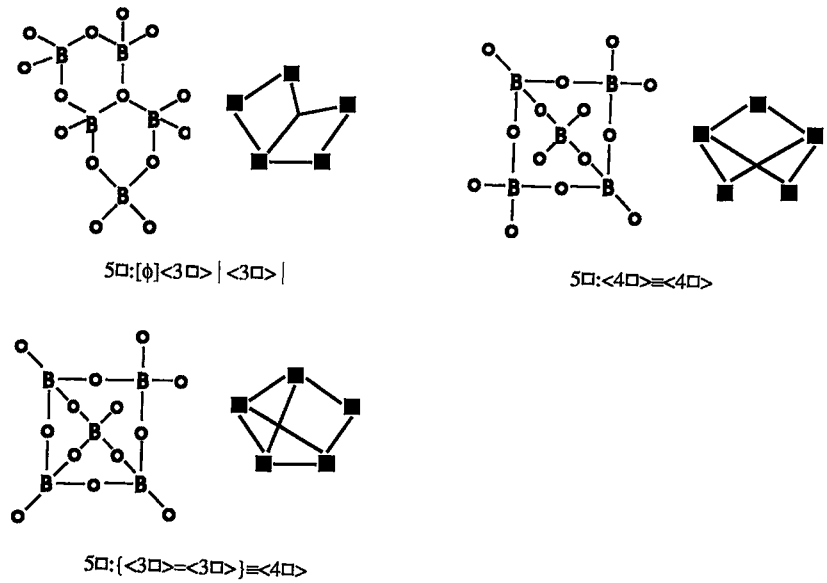

FIG. 4. The possible 2- or higher connected clusters for $3 \leq n \leq 5$ containing only □.

suitably modified for the presence of Δ and decorations where necessary.

Other possible clusters were obtained by permuting Δ for □ in the thirty-nine clusters of Figures 4 and 5. The graphs of the clusters for $3 \leq n \leq 5$ are given in Figure 6. In a later paper, we will examine possible factors that control the existence (or otherwise) of these clusters as FBBs in borate structures.

Fig. 5a

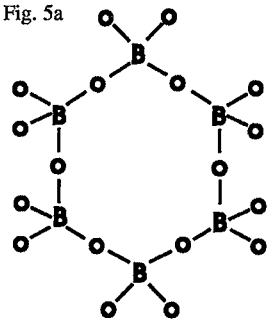

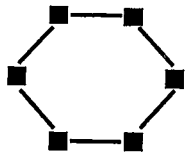

6□:<6□>

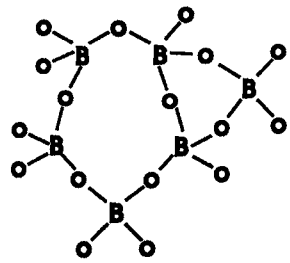

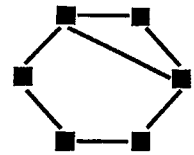

6□:<5□>=<3□>

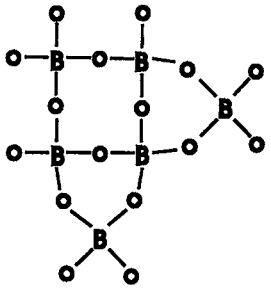

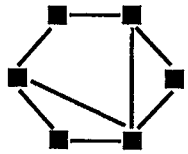

6□:<3□>=<4□>=<3□>

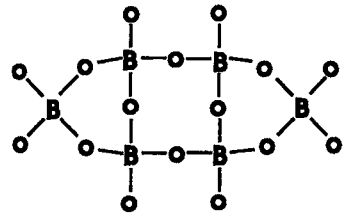

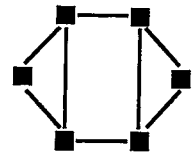

6□:<3□>=<4□>=<3□>

Fig. 5b

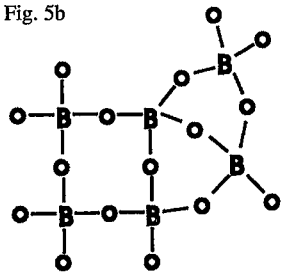

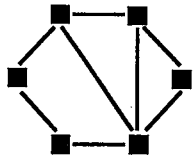

6□:<4□>=<3□>=<3□>

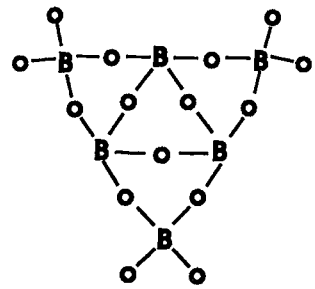

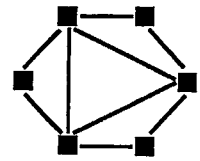

6□:[<3□>]=<3□>|=<3□>|=<3□>|

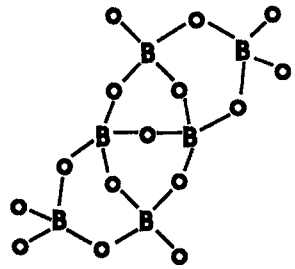

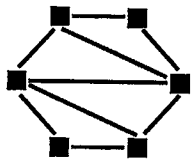

6□:<3□>=<3□>=<3□>=<3□>

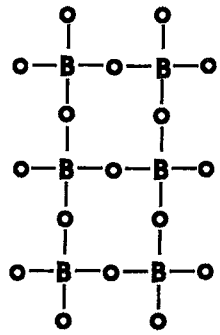

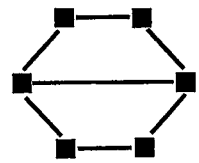

6□:<4□>=<4□>

Fig. 5c

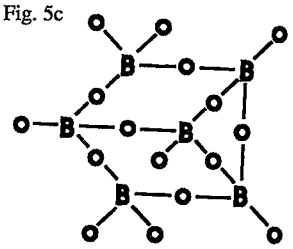

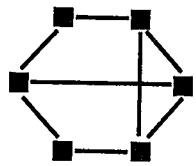

6□:{<4□>=<4□>}≡<3□>

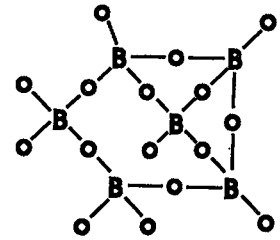

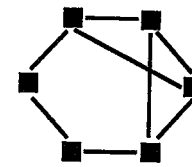

6□:{<3□>=<3□>}≡<5□>

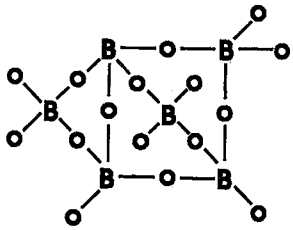

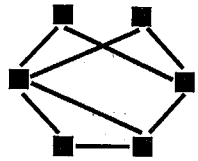

6□:<3□>={<4□>≡<4□>}

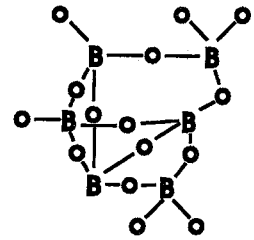

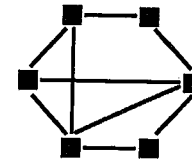

6□:{<3□>=<4□>=<3□>}≡<3□>

Fig. 5d

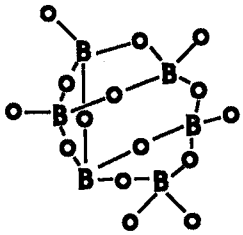

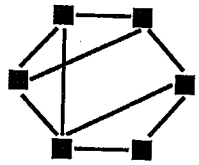

6□:{<3□>=<4□>=<3□>}≡<3□>

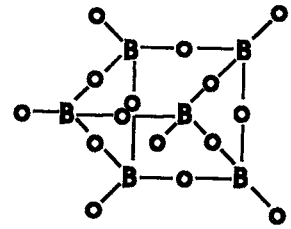

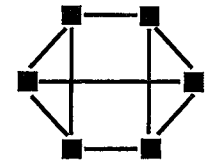

6□:<4□>≡{<3□>=<4□>=<3□>}≡<4□>

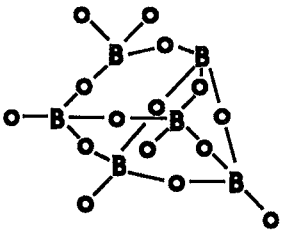

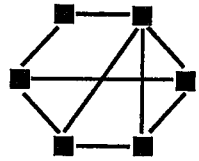

6□:<4□>≡{<3□>=<3□>=<4□>}≡<4□>

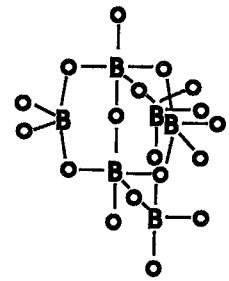

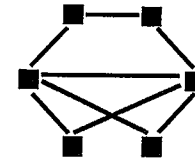

6□:{<3□>=<3□>}=<4□>

Fig. 5e

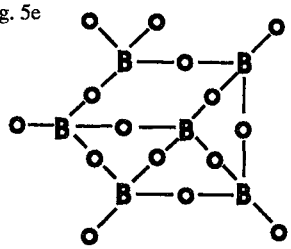

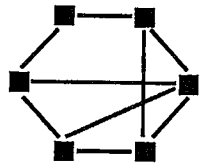

6□:{<3□>=<3□>=<4□>}≡<3□>

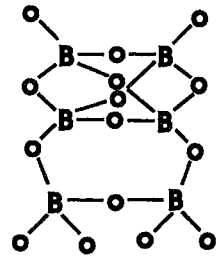

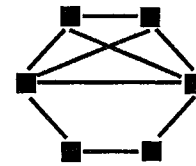

6□:{<3□>=<3□>=<4□>}≡<3□>

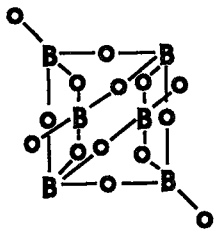

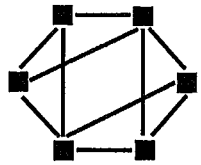

6□:<3□>≡{<3□>=<4□>=<3□>}≡<3□>

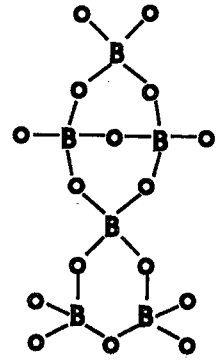

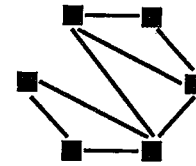

6□:<3□>-<3□>=<3□>

Fig. 5f

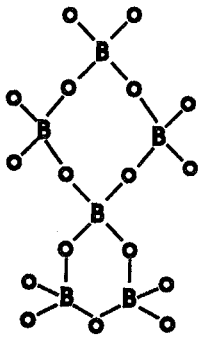

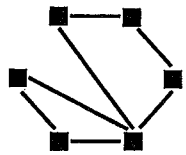

6□:<4□>-<3□>

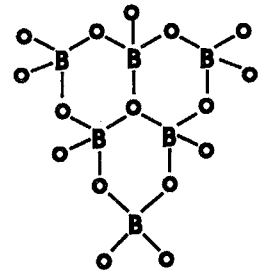

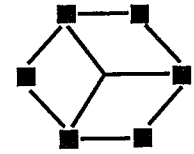

6□:[ϕ]<3□>|<3□>|<3□>|

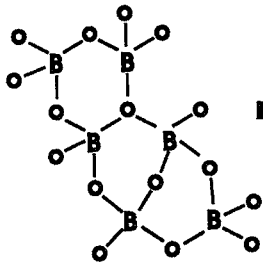

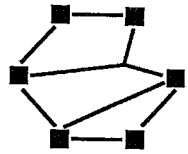

6□:[ϕ]<3□>|<3□>=<3□>|

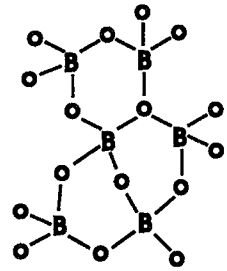

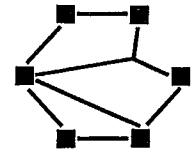

6□:[ϕ]<3□>|<3□>=<3□>|

Fig. 5g

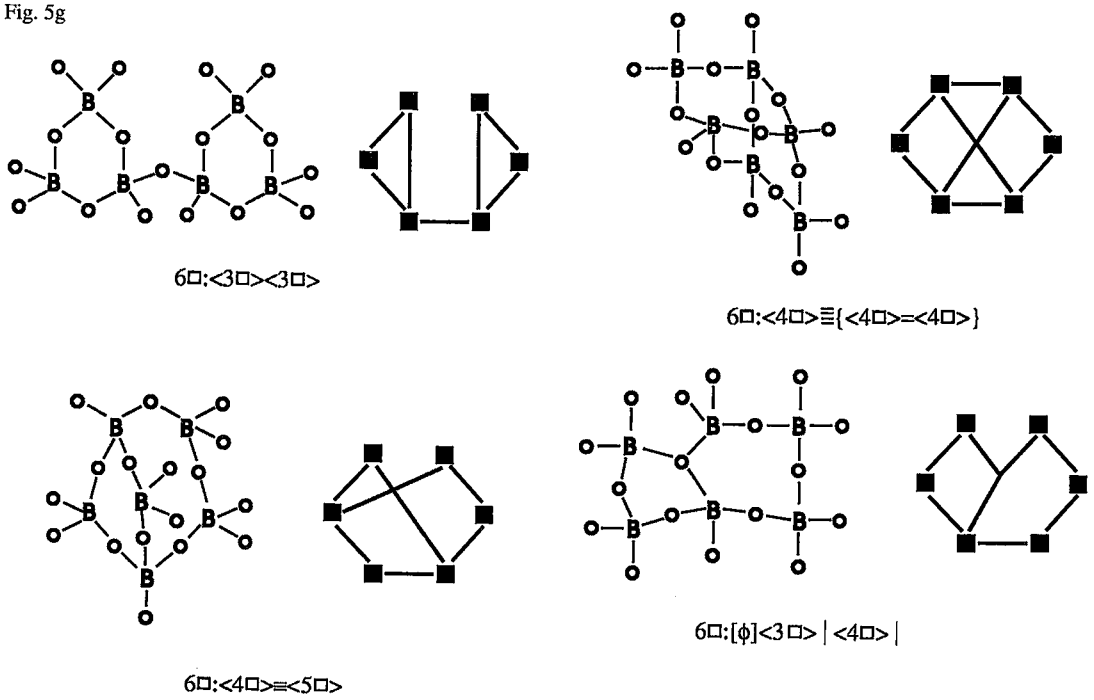

FIG. 5. The possible 2- or higher connected clusters for $n = 6$ containing only □.

THE OCCURRENCE OF FBBS IN THE STRUCTURES OF BORATE MINERALS

In the second paper of this series, we intend to arrange all borate minerals within a hierarchy of structures. In this paper, we restrict our discussion to the FBBs that occur in the structures of borate minerals, and ignore the overall connectivity of the structure. The purpose of what follows is the identification of FBBs that occur in mineral structures.

Graphical representation of all sterically possible $3 \le n \le 6$ clusters fall into thirty-nine sets if the coordination of the boron is ignored; these are given in Figures 4 and 5. We have identified fifty-one borate mineral structures with FBBs of $3 \le n \le 6$, and the frequency of occurrence of the eleven sets with $3 \le n \le 5$ is shown in Figure 7. In the case of $n = 6$, observed FBBs fall into two sets: 6B:[ϕ]<3B>|<3B>|<3B>| (11 occurrences) and 6B:<3B>=<4B>=<3B> (1 occurrence). The observed FBBs with $3 \le n \le 5$ fall into only four of the eleven sets, and only three of the sets have multiple examples. Borcarite is the only mineral that contains a FBB in the set 4B:<4B>. Inspection of Figure 7 shows that <3B> rings of polyhedra are dominant in FBBs; the 4□:<4□> FBB in borcarite is the *only* FBB that is not based on three-membered rings of polyhedra.

Within each set of clusters (Figs. 4, 5), there are several different possible FBBs with different numbers of Δ and □. The frequency of occurrence of each specific FBB within the three sets corresponding to 3B:<3B>, 4B:<3B>=<3B> and 5B:<3B>–<3B> is given in Figure 8. For $n = 6$, FBBs in the set 6B:[ϕ]<3B>|<3B>|<3B>| are of two kinds: ten are 3Δ3□:[ϕ]<Δ2□>|<Δ2□>|<Δ2□>|, and one is 6□:[ϕ]<3□>|<3□>|<3□>|. First, consider only those FBBs within the set 3B:<3B>. There are fourteen examples in minerals: nine are <Δ2□>, two are <3□>, two are <3Δ>, and one is <2Δ□>. Thus, for FBBs containing only one three-membered ring of polyhedra, the combination <Δ2□> seems favored relative to the other possible combinations.

Examination of larger FBBs shows that the <Δ2□> ring is a major component of these large clusters. In the FBB set 4B:<3B>=<3B>, all seven occurrences of the three-membered rings are <Δ2□>. In the FBB set 5B:<3B>–<3B>, there is more variability; of the nineteen examples, both of the three-membered rings are <Δ2□> in nine structures, one ring is <Δ2□> and the other is <2Δ□> in five structures, and in five structures neither of the rings is <Δ2□>. There are eleven examples in the FBB set 6B:[ϕ]<3B>|<3B>|<3B>|; in ten of these, all three of the rings of polyhedra are <Δ2□>, and only one does

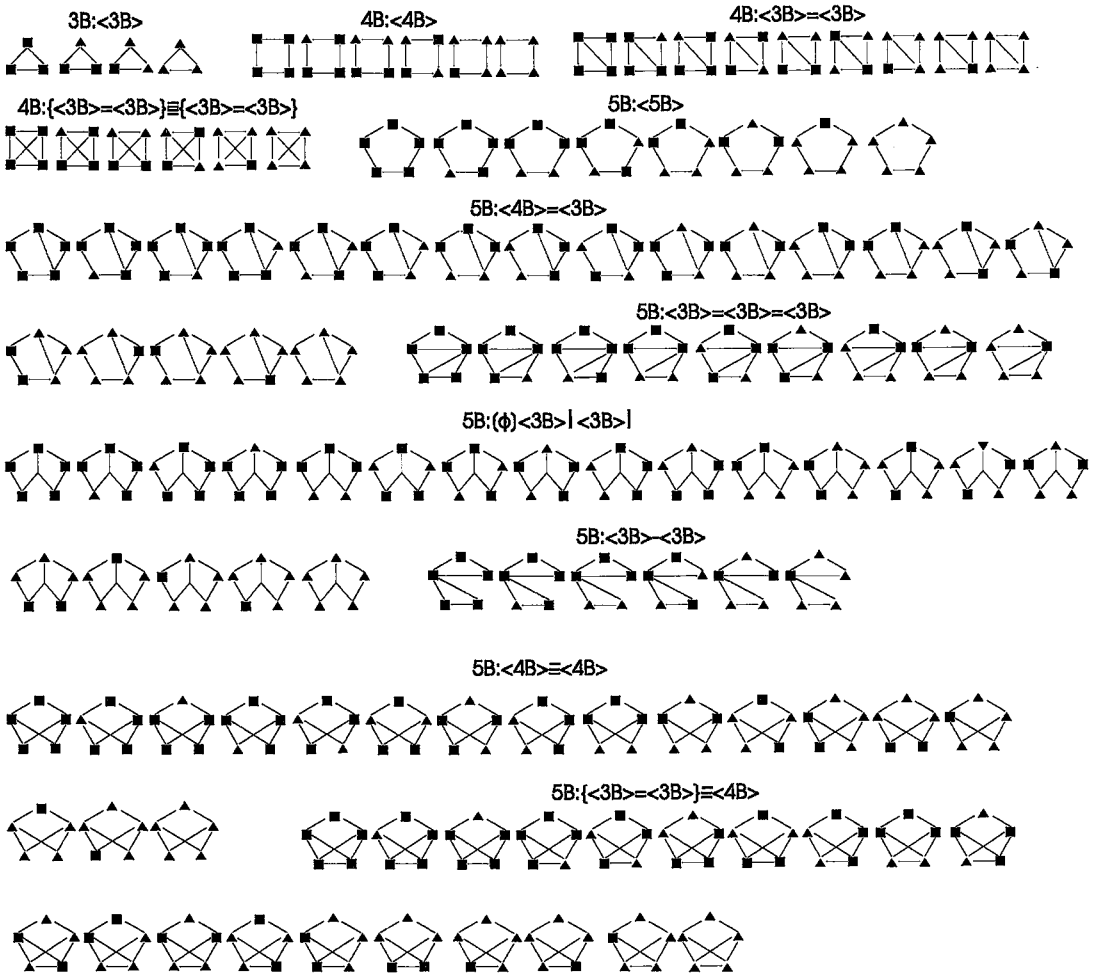

FIG. 6. All possible 2- or higher connected clusters for $n = 3, 4, 5$.

not contain a <Δ2□> ring.

The frequency of three-membered rings of polyhedra in borate structures is remarkable. Of the fifty-one borate minerals with $3 \le n \le 6$, *only one* FBB in *one* mineral is not based *solely* upon three-membered rings. In addition, thirty-five structures contain FBBs based *only* on the <Δ2□> three-membered ring, five contain FBBs based on three-membered rings of the form <Δ2□> and a ring of the form <2Δ□>, and only eleven (excluding borcarite) contain no <Δ2□> ring. We must conclude that <Δ2□> rings are strongly favored (energetically) in FBBs with $3 \le n \le 6$, and that the three-membered rings occur in the following order of preference: <Δ2□> >> <2Δ□> > <3□> > <3Δ>.

The origin of this preference is not readily apparent. Possible factors affecting the observed frequency of ring topologies are: (1) local bonding effects within the ring may make the <Δ2□> ring more stable than other three-membered or n-membered rings, (2) long-range structural effects may favor the inclusion of <Δ2□> rings rather than the other possibilities, and (3) the <Δ2□> ring may be favored in the precursor fluid medium (under certain pH, Eh conditions), thereby making it more readily available for incorporation into a growing crystal. We are currently investigating local bonding effects in borate clusters using molecular-orbital calculations.

Many clusters with $3 \le n \le 6$ (Figs. 4, 5) include rings other than the favored three-membered rings, and

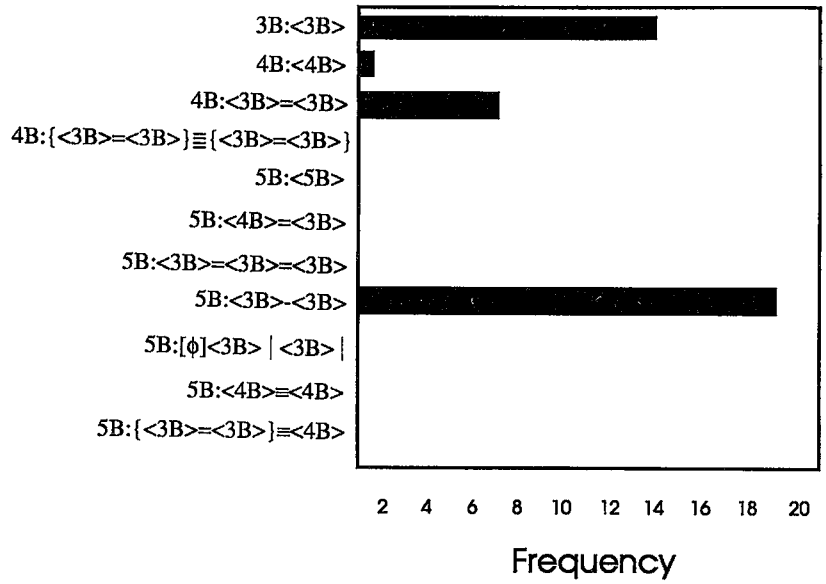

FIG. 7. The frequency of occurrence of each of the eleven classes of clusters ($3 \leq n \leq 5$) in borate mineral structures.

with the exception of the FBB 4□:<4□> in borcarite, none of these have been observed in mineral structures. However, there are also several sets of clusters with $3 \leq n \leq 6$ that contain only three-membered rings (Figs. 4, 5) that have not yet been found in any borate mineral structure.

SUMMARY

(1) We have developed a new representation and descriptor for borate clusters that includes information on the total number of boron atoms, the coordination of the boron atoms (Δ: triangular, □: tetrahedral), the connectivity of Δ and □, the presence of rings, and the connectivity within and between the rings.
(2) We have derived all clusters that are at least [2]-connected, but not more than [4]-connected, which have three to six polyhedra.
(3) In the structures of borate minerals containing borate FBBs with $3 \leq n \leq 6$, FBBs incorporating only three-membered rings of polyhedra are almost dominant. One FBB that is a four-membered ring of polyhedra is known (in borcarite).
(4) Three-membered rings of polyhedra occur in borate mineral structures in the following order of preference: <Δ2□> >> <2Δ□> > <3□> > <3Δ>.

ACKNOWLEDGEMENTS

This work was supported by the Natural Sciences and Engineering Research Council of Canada *via* a Post-Doctoral Fellowship to PCB and an Operating Grant to FCH. Clare Hall, Cambridge, supported this work *via* a research fellowship to PCB. Reviews of an earlier version of this manuscript by Drs. Paul B. Moore and John M. Hughes, and editorial work by R.F. Martin, were invaluable in preparing this manuscript.

REFERENCES

BEHM, H. (1983): Hexasodium (*cyclo*-decahydroxotetracosaoxohexadeca-borato)dicuprate(II) dodecahydrate, $Na_6[Cu_2\{B_{16}O_{24}(OH)_{10}\}]\cdot 12H_2O$. *Acta Crystallogr.* **C39**, 20-22.

_____ (1985): Hexapotassium (*cyclo*-octahydroxotetracosaoxohexadeca-borato)dioxouranate(VI) dodecahydrate, $K_6[UO_2\{B_{16}O_{24}(OH)_8\}]\cdot 12H_2O$. *Acta Crystallogr.* **C41**, 642-645.

BRAGG, W.L. (1930): The structure of silicates. *Z. Kristallogr.* **74**, 237-305.

BROWN, I.D. (1981): The bond-valence method: an empirical approach to chemical structure and bonding. *In* Structure and Bonding in Crystals II (M. O'Keeffe & A. Navrotsky, eds.) Academic Press, New York, N.Y. (1-30).

BRUALDI, R.A. (1991): *Combinatorial Matrix Theory.* Cambridge University Press, Cambridge, U.K.

BURDETT, J.K. (1986): Structural-electronic relationships in the solid state. *Mol. Struct. Energ.* **1**, 209-275.

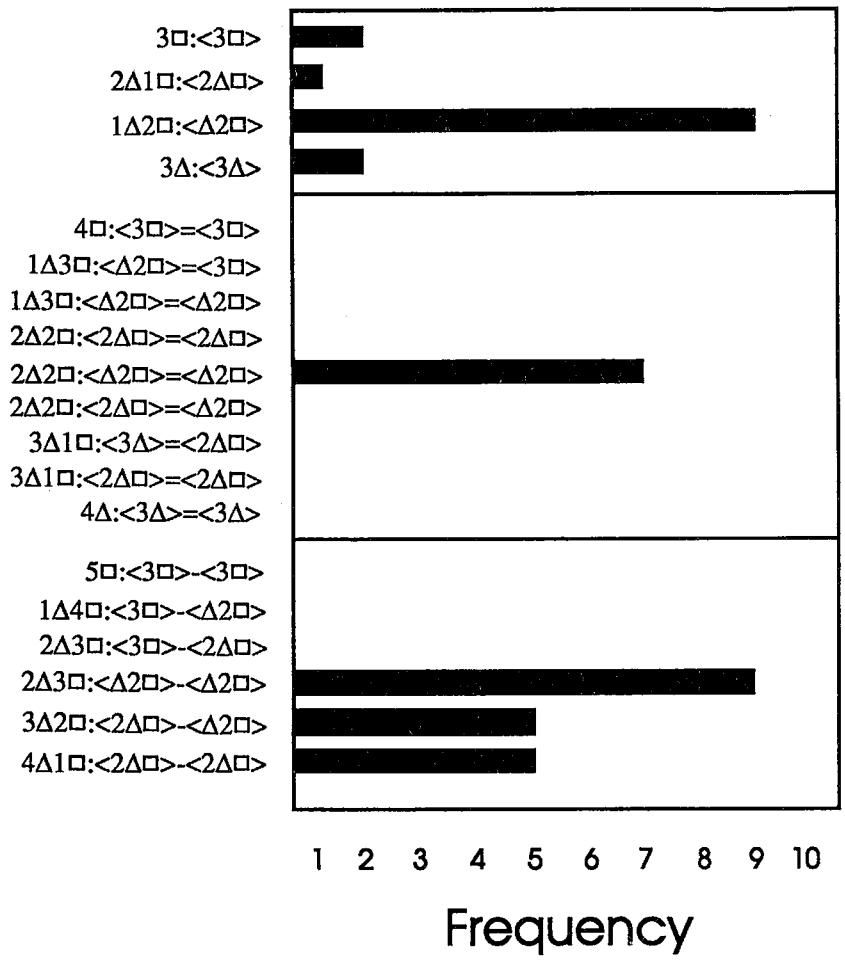

FIG. 8. The frequency of occurrence of selected clusters as FBBs in borate mineral structures.

BURNS, P.C. & HAWTHORNE, F.C. (1993a): Hydrogen bonding in colemanite: an X-ray and structure-energy study. *Can. Mineral.* **31**, 297-304.

_____ & _____ (1993b): Hydrogen bonding in meyerhofferite: an X-ray and structure energy study. *Can. Mineral.* **31**, 305-312.

_____ & _____ (1994a): Hydrogen bonding in tunellite. *Can. Mineral.* **32** 895-902.

_____ & _____ (1994b): Structure and hydrogen bonding in preobrazhenskite, a complex heteropolyhedral borate. *Can. Mineral.* **32**, 387-396.

_____ & _____ (1994c): Structure and hydrogen bonding in inderborite, a heteropolyhedral sheet structure. *Can. Mineral.* **32**, 533-539.

_____ & _____ (1994d): Kaliborite: an example of a crystallographically symmetrical hydrogen bond. *Can. Mineral.* **32**, 885-894.

_____ & _____ (1995): Hydrogen bonding in borcarite, an unusual carbo-borate mineral. *Mineral. Mag.* **59**, 297-304.

CHRIST, C.L. (1960): Crystal chemistry and systematic classification of hydrated borate minerals. *Am. Mineral.* **45**, 334-340.

_____ & CLARK, J.R. (1977): A crystal-chemical classification of borate structures with emphasis on hydrated borates. *Phys. Chem. Minerals* **2**, 59-87.

COHEN, D.I.A. (1978): *Basic Techniques of Combinatorial Theory*. Wiley, New York, N.Y.

EDWARDS, J.O. & ROSS, V.F. (1960): Structural principles of the hydrated polyborates. *J. Inorg. Nucl. Chem.* **15**, 329-337.

GRICE, J.D., BURNS, P.C. & HAWTHORNE, F.C. (1994): Determination of the megastructures of the borate polymorphs pringleite and ruitenbergite. *Can. Mineral.* **32**, 1-14.

HAWTHORNE, F.C. (1983): Graphical enumeration of polyhedral clusters. *Acta Crystallogr.* **A39**, 724-736.

_____ (1984): The crystal structure of stenonite and the classification of the aluminofluoride minerals. *Can. Mineral.* **22**, 245-251.

_____ (1985): Towards a structural classification of minerals: the $^{vi}M^{iv}T_2\phi_n$ minerals. *Am. Mineral.* **70**, 455-473.

_____ (1990): Structural hierarchy in $M^{[6]}(T^{[4]}\phi_n)$ minerals. *Z. Kristallogr.* **192**, 1-52.

_____ (1994): Structural aspects of oxide and oxysalt crystals. *Acta Crystallogr.* **B50**, 481-510.

HELLER, G. (1970): Darstellung und Systematisierung von Boraten und Polyboraten. *Fortschr. Chem. Forschung* **15**, 206-280.

_____ & PICKARDT, J. (1985): Über ein Ikosaborat-ion in hydratisierten Kalium- und Natriumkupferpolyboraten. *Z. Naturforsch.* **40b**, 462-466.

LIEBAU, F. (1985): *Structural Chemistry of Silicates.* Springer-Verlag, Berlin, Germany.

MENCHETTI, S. & SABELLI, C. (1979): A new borate polyanion in the structure of $Na_8[B_{12}O_{20}(OH)_4]$. *Acta Crystallogr.* **B35**, 2488-2493.

MOORE, P.B. (1965): A structural classification of Fe–Mn orthophosphate hydrates. *Am. Mineral.* **50**, 2052-2062.

_____ (1973): Pegmatite phosphates: descriptive mineralogy and crystal chemistry. *Mineral. Rec.* **4**, 103-130.

ROSS, V.F. & EDWARDS, J.O. (1967): The structural chemistry of the borates. *In* The Chemistry of Boron and its Compounds (E.L. Muetterties, ed.). John Wiley, New York, N.Y. (155-207).

SHANNON, R.D. (1976): Revised effective ionic radii and systematic studies of interatomic distances in halides and chalcogenides. *Acta Crystallogr.* **A32**, 751-767.

SKAKIBAIE-MOGHADAM, M., HELLER, G. & TIMPER, U. (1990): Die Kristallstruktur von $Ag_6[B_{12}O_{18}(OH)_6]\cdot 3H_2O$, einem neuen Dodekaborat. *Z. Kristallogr.* **190**, 85-96.

SMITH, J.V. (1977): Enumeration of 4-connected 3-dimensional nets and classification of framework silicates. I. Perpendicular linkage from simple hexagonal net. *Am. Mineral.* **62**, 703-709.

_____ (1988): Topochemistry of zeolites and related materials. 1. Topology and geometry. *Chem. Rev.* **88**, 149-182.

SUENO, S., CLARK, J.R., PAPIKE, J.J. & KONNERT, J.A. (1973): Crystal-structure refinement of cubic boracite. *Am. Mineral.* **58**, 691-697.

TENNYSON, C. (1963): Eine Systematik der Borate auf kristallchemischer Grundlage. *Fortschr. Mineral.* **41**, 64-91.

ZOLTAI, T. (1960): Classification of silicates and other minerals with tetrahedral structures. *Am. Mineral.* **45**, 960-973.

Received December 8, 1994, revised manuscript accepted April 6, 1995.

APPENDIX I

Consider the B–B graph shown in Figure A1; let us call this graph G. This is a labeled graph in which vertices represent borate polyhedra of unspecified type, and edges represent linkage between these polyhedra such that the polyhedral cluster represented consists of two three-membered rings with two polyhedra in common. The problem is to determine how many distinct clusters of borate triangles and tetrahedra are possible; this reduces to determining how many distinct black (tetrahedron, □) and white (triangle, Δ) colorings of the graph in Figure A1 are distinct.

The automorphism group, P, of a graph is the collection of all permutations of the vertex labelings that preserve isomorphism. The collection of all possible permutations of the vertex labelings is the symmetric group S_n (where $n = 4$ in Fig. A1). P is a subgroup of S_n, and the complementary disjoint subgroup of S_n defines all labelings of the graph G that are distinct. The disjoint cycle decomposition and cycle structure of P for G of Figure A1 is given in Table A1. The corresponding cycle index of G, denoted $Z(P)$ is given by

$$Z(P) = \frac{1}{|P|} \sum_{p \in P} \prod_{k=1}^{N} s_k^{j(k,p)} = \frac{1}{4}\left[s_1^4 + 2s_2^1 + s_2^2\right] \quad \text{(A1)}$$

following standard nomenclature in combinatorial theory (Brualdi 1991, Cohen 1978). From the unweighted version of Pólya's theorem, the number of distinct schemes, $|S|$, is given by $Z(P:m)$, that is, by substitution of the number of different colors (*i.e.*, □ or Δ: $m = 2$) for the dummy variable $s_k^{j(k,p)}$:

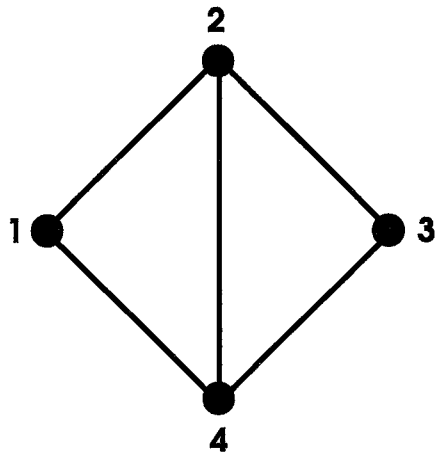

FIG. A1. A labeled B–B graph, G, in which the vertices represent polyhedra and the edges denote linkage between polyhedra.

TABLE A1. DISJOINT CYCLE DECOMPOSITION AND CYCLE STRUCTURE OF THE AUTOMORPHISM GROUP P OF THE GRAPH G IN FIGURE A1

Disjoint cycle decomposition	Cycle structure*
(1) (2) (3) (4)	s_1^4
(2) (4) (1 3)	$s_1^2 s_2^1$
(1) (3) (2 4)	$s_1^2 s_2^1$
(1 3) (2 4)	s_2^2

* s are dummy variables that carry the cycle structure of the disjoint cycle decomposition.

$$|S| = \frac{1}{4}\left[2^4 + 2 \cdot 2^2 \cdot 2 + 2^2\right] = 9 \quad \text{(A2)}$$

There are thus nine distinct possible arrangements of four borate polyhedra that consist of two three-membered rings with two polyhedra in common.

APPENDIX II

We wish to derive all geometrically possible clusters of n tetrahedra (specifically for $n = 4$ to $n = 6$) subject to the condition that tetrahedra link by sharing corners only and that each oxygen is not bonded to more than two boron atoms. We will begin by deriving all topologically possible clusters, and then will discard those clusters in which the tetrahedra are interpenetrant, deformed beyond chemical feasibility, are not at least two-connected, are greater than four-connected, or which form disconnected rings. The linkage between polyhedra is defined by the edge set of the corresponding graph, and hence we are concerned with the combinatorial characteristics of the edge set of the graph. First, it is necessary to emphasize that this is a topological problem rather than a geometrical problem (as was the case in Appendix I). Hence the relevant automorphism group for the vertex set is the symmetric group S_n. This has a corresponding permutation group, P_N [$N = n(n-1)/2$], that permutes the edge set, and it is the cycle structure of P_N that can be used, together with the weighted version of Pólya's theorem, to calculate the inventory of topologically distinct arrangements. A convenient way to deal with the structure of the edge set is to allow the operations of S_n to permute the elements of the vertex set, and to derive the corresponding operations of P_N by examining the resulting structure of the adjacency matrix.

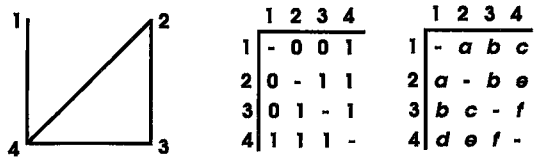

FIG. A2. A graph with $n = 4$ (left), the adjacency matrix for the graph (middle), and the corresponding general adjacency matrix (right).

Figure A2 shows a specific graph with $n = 4$, the adjacency matrix of that graph, and the corresponding general adjacency matrix that we use here.

Consider first the case for $n = 4$. The disjoint cycle decomposition and elements of the cycle structure for S_4 are shown in Table A2, together with the corresponding elements for P_N. The resulting cycle structure for P_6 is thus

$$Z(P_6) = \frac{1}{24}\,[s_1^6+9s_1^2s_2^2+8s_3^2+6s_2^1s_4^1] \qquad \text{(A3)}$$

The number of distinct arrangements, $|S|$, can now be derived from the unweighted version of Pólya's theorem by substituting the number of possible values, m, of the matrix elements for s_i in the cycle structure:

$$|S| = Z(P{:}m) = \frac{1}{24}\,[m^6+9m^4+14m^2] \qquad \text{(A4)}$$

TABLE A2. DISJOINT CYCLE DECOMPOSITIONS AND CYCLE STRUCTURES OF S_4 AND P_6

Disjoint cycle decomposition of S_4	Cycle structure	Disjoint cycle decomposition of P_6	Cycle structure
(1) (2) (3) (4)	s_1^4	(*a*) (*b*) (*c*) (*d*) (*e*) (*f*)	s_1^6
(1 2) (3) (4)	$s_1^2 s_2^1$	(*a*) (*b c*) (*d e*) (*f*)	$s_1^2 s_2^2$
(1 3) (2) (4)	$s_1^2 s_2^1$	(*a c*) (*b*) (*d f*) (*e*)	$s_1^2 s_2^2$
(1 4) (2) (3)	$s_1^2 s_2^1$	(*a e*) (*b f*) (*c*) (*d*)	$s_1^2 s_2^2$
(1) (2 3) (4)	$s_1^2 s_2^1$	(*a b*) (*c*) (*d*) (*e f*)	$s_1^2 s_2^2$
(1) (2 4) (3)	$s_1^2 s_2^1$	(*a d*) (*b*) (*c f*) (*e*)	$s_1^2 s_2^2$
(1) (2) (3 4)	$s_1^2 s_2^1$	(*a*) (*b d*) (*c e*) (*f*)	$s_1^2 s_2^2$
(1 2) (3 4)	s_2^2	(*a*) (*b e*) (*c d*) (*f*)	$s_1^2 s_2^2$
(1 3) (2 4)	s_2^2	(*a f*) (*b*) (*c d*) (*e*)	$s_1^2 s_2^2$
(1 4) (2 3)	s_2^2	(*a f*) (*b e*) (*c*) (*d*)	$s_1^2 s_2^2$
(1 2 3) (4)	$s_1^1 s_3^1$	(*a b c*) (*d f e*)	s_3^2
(1 3 2) (4)	$s_1^1 s_3^1$	(*a c b*) (*d e f*)	s_3^2
(1 2 4) (3)	$s_1^1 s_3^1$	(*a d e*) (*b f c*)	s_3^2
(1 4 2) (3)	$s_1^1 s_3^1$	(*a e d*) (*b c f*)	s_3^2
(1 3 4) (2)	$s_1^1 s_3^1$	(*a e c*) (*b d f*)	s_3^2
(1 4 3) (2)	$s_1^1 s_3^1$	(*a c e*) (*b f d*)	s_3^2
(1) (2 3 4)	$s_1^1 s_3^1$	(*a d b*) (*c e f*)	s_3^2
(1) (2 4 3)	$s_1^1 s_3^1$	(*a b d*) (*c f e*)	s_3^2
(1 2 3 4)	s_4^1	(*a d f c*) (*b e*)	$s_2^1 s_4^1$

The elements of the adjacency matrix, $\{a, b \ldots f\}$, can be chosen from the set $\{0,1\}$, indicating no linkage or linkage, respectively, between tetrahedra. Thus $m = 2$ and

$$|S| = \frac{1}{24}\,[2^6+9\cdot2^4+14\cdot2^2] = 11 \qquad \text{(A5)}$$

Thus there are 11 topologically distinct clusters for $n = 4$. We may derive information on their structure by using the weighted version of Pólya's theorem. The matrix elements $\{a, b \ldots f\}$ are chosen from the set $\{0,1\}$; let us assign weights $\{u,v\}$ to the set $\{0,1\}$. We can then derive the inventory of arrangements, inv$|S|$, by substituting the weight functions

$$w_k = \sum_{r=1}^{k} w(r)^k = u^k+v^k \quad k=1,n \qquad \text{(A6)}$$

for the dummy variables $s_k^{j(k,p)}$ in the cycle index. The resulting inventory of arrangements is

$$\begin{aligned} inv|S| &= \frac{1}{24}\,[(u+v)^6+9(u+v)^2(u^2+v^2)^2+8(u^3+v^3)^2 \\ &\qquad +6(u^2+v^2)\,(u^4+v^4)] \\ &= u^6+u^5v+2u^4v^2+3u^3v^3+2u^2v^4+uv^5+v^6 \end{aligned} \qquad \text{(A7)}$$

Each term in the inventory corresponds to a certain number of edges, and the coefficient of each term denotes how many topologically distinct arrangements occur with that number of edges; thus the term $2u^4v^2$ indicates that there are two distinct arrangements with two ($v = 2$) edges. Now we require that all vertices be at least two-connected; a necessary-but-not-sufficient condition for this is that there be at least four edges in the graphs, and this means that we are only concerned with inventory terms for which the exponent of v is greater than or equal to 4 (*i.e.*, n, the number of vertices in the vertex set of the graph): $2u^2v^4$, uv^5 and v^6. These graphs are shown in Figure A3. Note that one of the

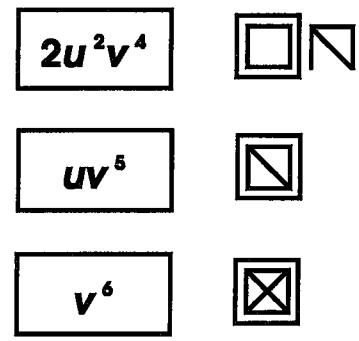

FIG. A3. Graphs for possible borate clusters with $n = 4$ that contain at least four vertices. Boxes are drawn around the graphs of interest, *i.e.*, those that are at least two-connected and are not greater than four-connected.

arrangements has a one-connected vertex, and hence is not needed; the other three graphs are relevant, and the resulting clusters are shown in Figure 4.

Having illustrated the method, we can now take a short cut in the calculations for $n = 5$ and $n = 6$. The different permutations of S_n can be divided up into conjugacy classes, the structure of which is denoted by the symbol

$$\prod_{k=1}^{n} s_k^{j(k,g)} \qquad \text{(A8)}$$

TABLE A3. CYCLE STRUCTURES AND NUMBER OF ELEMENTS IN S_n AND $P_{n(n+1)/2}$ FOR $n = 5$ AND 6

Cycle structure		Cycle structure
S_5	N*	P_{10}
s_1^5	1	s_1^{10}
$s_1^3 s_2^1$	10	$s_1^4 s_2^3$
$s_1^1 s_2^2$	15	$s_1^2 s_2^4$
$s_1^2 s_3^1$	20	$s_1^1 s_3^3$
$s_2^1 s_3^1$	20	$s_1^1 s_3^1 s_6^1$
$s_1^1 s_4^1$	30	$s_2^1 s_4^2$
s_6^1	24	s_5^2
S_6	N*	P_{15}
s_1^6	1	s_1^{15}
$s_1^4 s_2^1$	15	$s_1^7 s_2^4$
$s_1^2 s_2^2$	45	$s_1^3 s_2^6$
s_2^3	15	$s_1^3 s_2^6$
$s_1^3 s_3^1$	40	$s_1^3 s_3^4$
$s_1^1 s_2^1 s_2^1$	120	$s_1^1 s_2^1 s_3^2 s_6^1$
s_3^2	40	s_3^5
$s_1^2 s_4^1$	90	$s_1^1 s_2^1 s_4^3$
$s_2^1 s_4^1$	90	$s_1^1 s_2^1 s_4^3$
$s_1^1 s_5^1$	144	s_5^3
s_6^1	120	$s_3^1 s_6^2$

*N = number of elements of S_n (and $P_{n(n-1)/2}$) with the cycle structure indicated

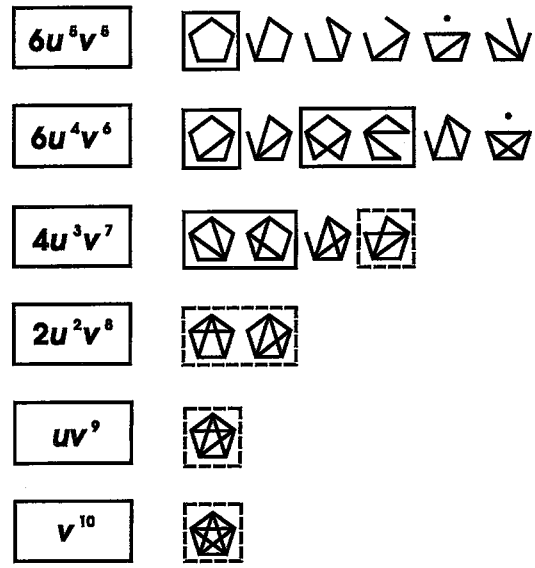

FIG. A4. Graphs for possible borate clusters with $n = 5$ that contain at least five vertices. Boxes are drawn around the graphs of interest, *i.e.*, those that are at least two-connected and are not greater than four-connected. Where the graphs meet these criteria but are deformed beyond chemical feasibility, or contain interpenetrant tetrahedra or disjoint rings, the boxes are drawn using broken lines.

in which $s_k^{j(k,g)}$ are the dummy variables used above, and $j(k,g)$ denotes j cycles of length k in the permutation $g \in S_n$. The number of conjugacy classes in S_n is $p(n)$, the number of partitions of the integer n. Thus we can derive the conjugacy-class structure of S_n from $p(n)$; the corresponding cycle index of S_n is thus the sum of the elements of the conjugacy class of S_n, each multiplied by an appropriate coefficient that denotes the number of disjoint cycle decompositions of S_n with that specific cycle-structure. The conjugacy classes of S_5 and S_6 are shown in Table A3. How do we derive the appropriate coefficients? For a specific cycle structure [*e.g.*, $s\ s$ for S_5: a specific example is (1 2 3)(4 5)], we calculate the number of distinct arrangements [for $s\ s$ {*e.g.*, (1 2 3)(4 5)}: in this case, the number of distinct arrangements is $5 \times 4 \times 3/3$ for s and $2 \times 1/2$ for s, and the total number is therefore $5 \times 4 \times 3 \times 2/3 \times 2 = 20$]. The resultant values for S_5 and S_6 are given in Table A3. Now although the conjugacy classes of P_N are different from those of S_n, corresponding conjugacy classes in the cycle indices of each group must have the same coefficient, and each operation in S_n has a corresponding operation in P_N. Thus, to derive the complete cycle index for P_N, we need only to derive

the cycle structure for one operation within each conjugacy class. The corresponding conjugacy classes and associated coefficients for P_{10} (associated with S_5) and P_{15} (associated with S_6) are given in Table A3. From Table A3, we can write down the cycle structures for P_{10} and P_{15}, and proceed with calculating the pattern inventory as was done above for $n = 4$.

For $n = 5$, the resulting cycle structure for P_{10} is

$$Z(P) = \frac{1}{120}[s_1^{10}+10s_1^4s_2^3+15s_1^2s_2^4+20s_1^1s_3^3 +20s_1^1s_3^1s_6^1+30s_2^1s_4^2+24s_5^2] \quad (A9)$$

The total number of distinct arrangements is given by $Z(P{:}2)$:

$$Z(P{:}2) = \frac{1}{120}[2^{10}+10{\cdot}2^4{\cdot}2^3+15{\cdot}2^2{\cdot}2^4+20{\cdot}2{\cdot}2^3 +20{\cdot}2{\cdot}2{\cdot}2+30{\cdot}2{\cdot}2^2+24{\cdot}2^2] = 34 \quad (A10)$$

The corresponding pattern inventory is given by

$$\begin{aligned} inv|S| = \frac{1}{120}&[(u+v)^{10}+10(u+v)^4(u^2+v^2)^3 \\ &+15(u+v)^2(u^2+v^2)^4+20(u+v)(u^3+v^3)^3 \\ &+20(u+v)(u^3+v^3)(u^6+v^6) \\ &+30(u^2+v^2)(u^4+v^4)^2+24(u^5+v^5)^2] \\ &= u^{10}+u^9v+2u^8v^2+4u^7v^3+6u^6v^4+6u^5v^5 \\ &+6u^4v^6+4u^3v^7+2u^2v^8+uv^9+v^{10} \end{aligned} \quad (A11)$$

Requiring that all vertices be two-connected is a necessary-but-not-sufficient condition that restricts our interest to arrangements with the exponent of v equal to or greater than 5; these 20 graphs are shown in Figure A4. Nine of the 20 graphs have a zero- or one-connected vertex; five graphs require very highly distorted or interpenetrant tetrahedra. The remaining six graphs are geometrically possible, and are represented in Figure 4.

For $n = 6$, the cycle structure for P_{15} is

$$\begin{aligned} Z(P) = \frac{1}{720}&[s_1^{15}+15s_1^7s_2^4+60s_1^3s_2^6+40s_1^3s_3^4 \\ &+180s_1^1s_2^1s_3^3+120s_1^1s_2^1s_3^2s_6^1+40s_3^5 \\ &+144s_5^3+120s_3^1s_6^2] \end{aligned} \quad (A12)$$

The total number of distinct arrangements is given by $Z(P{:}2)$:

$$Z(P{:}2) = \frac{1}{120}[2^{15}+15{\cdot}2^{11}+60{\cdot}2^9+40{\cdot}2^7+120{\cdot}2^5 +40{\cdot}2^5+144{\cdot}2^3+120{\cdot}2^3] = 156 \quad (A13)$$

The corresponding pattern inventory is given by

$$\begin{aligned} inv|S| = \frac{1}{170}&[(u+v)^{15}+15\,(u+v)^7\,(u^2+v^2)^4 \\ &+60\,(u+v)^3\,(u^2+v^2)^6+40\,(u+v)^3\,(u^3+v^3)^4 \\ &+180\,(u+v)\,(u^2+v^2)\,(u^4+v^4)^3 \\ &+120\,(u+v)\,(u^2+v^2)\,(u^3+v^3)^2\,(u^6+v^6) \\ &+40\,(u^3+v^3)^5+144\,(u^5+v^5)^3 \\ &+120\,(u^3+v^3)\,(u^6+v^6)^2] \\ &= u^{15}+u^{14}v+2u^{13}v^2+5u^{12}v^3+9u^{11}v^4 \\ &+15u^{10}v^5+21u^9v^6+24u^8v^7+24u^7v^8 \\ &+21u^6v^9+15u^5v^{10}+9u^4v^{11}+5u^3v^{12} \\ &+2u^2v^{13}+uv^{14}+v^{15} \end{aligned} \quad (A14)$$

Requiring that all vertices are two-connected is a necessary-but-not-sufficient condition that restricts our attention to arrangements with the exponent of v equal to or greater than 6. Exponents of v greater than 12 must involve arrangements with at least one five-connected vertex and can be discounted. As can be read from the above pattern inventory, there are 119 relevant arrangements; these are shown in Figure A5. Geometrically possible clusters are shown in Figure 5.

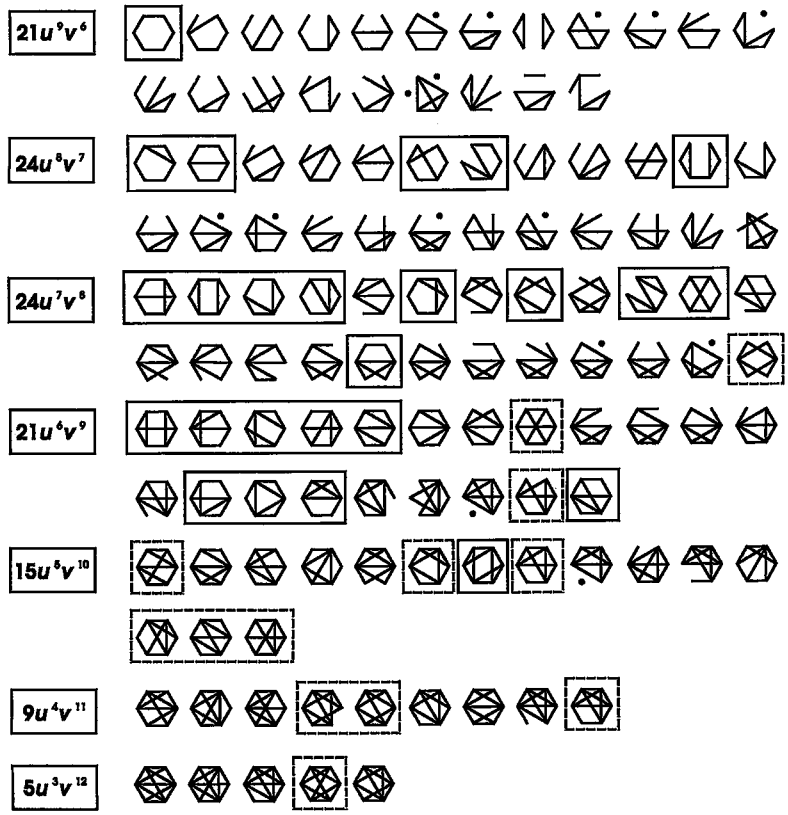

FIG. A5. Graphs for possible borate clusters with $n = 6$ that contain at least six vertices. Boxes are drawn around the graphs of interest, *i.e.*, those that are at least two-connected and are not greater than four-connected. Where the graphs meet these criteria but are deformed beyond chemical feasibility, or contain interpenetrant tetrahedra or disjoint rings, the boxes are drawn using broken lines.